 CMES, vol.108, no.4, pp.215-237, 2015

Meshless Local Petrov-Galerkin Method for Rotating Timoshenko Beam: a Locking-Free Shape Function Formulation

V. Panchore[1], R. Ganguli[2], S. N. Omkar[3]

Abstract: A rotating Timoshenko beam free vibration problem is solved using the meshless local Petrov-Galerkin method. A locking-free shape function formulation is introduced with an improved radial basis function interpolation and the governing differential equations of the Timoshenko beam are used instead of the alternative formulation used by Cho and Atluri (2001). The locking-free approximation overcomes the problem of ill conditioning associated with the normal approximation. The radial basis functions satisfy the Kronercker delta property and make it easier to apply the essential boundary conditions. The mass matrix and the stiffness matrix are derived for the meshless local Petrov-Galerkin method. Results are validated for the fixed-free boundary condition with published literature.

Keywords: Meshless local petrov-galerkin method; Radial basis function; Rotating timoshenko beam; Finite element method; Free vibration.

1 Introduction

The meshless methods show considerable improvements over the conventional finite element method: remeshing of the structure is avoided, the problem of large deformation can be addressed properly whereas in the finite element procedure elements get distorted, and higher order derivatives of field variable are continuous. The meshless local Petrov-Galerkin method is a truly meshless method, which does not require any background mesh while integrating the weak form of an equation [Atluri et al. (2013)]. The meshless Petrov-Galerkin method is suitable for various

[1] Ph.D. Student, Department of Aerospace Engineering, Indian Institute of Science, Bangalore, India, Email: vijaypanchore@aero.iisc.ernet.in

[2] Professor, Department of Aerospace Engineering, Indian Institute of Science, Bangalore, India, Email: ganguli@aero.iisc.ernet.in

[3] Chief Research Scientist, Department of Aerospace Engineering, Indian Institute of Science, Bangalore, India, Email: omkar@aero.iisc.ernet.in

combinations of test functions and trial functions [Atluri and Shen (2002); Atluri (2004)].

The rotating Timoshenko beam analytical solutions are difficult to obtain and the semi-analytical solutions were obtained using the power series method [Stafford and Giurgiutiu (1975); Du, Lim, and Liew (1994); Banerjee (2001)]. The Timoshenko rotating beam free vibration problem was solved using the finite element method [Yokoyama (1988); Rao and Gupta (2001)]. An additional term $\rho I\Omega^2\theta$ was included in the Timoshenko rotating beam formulation, which does make a contribution at the high rotational speed and the differential transform method was used to solve the free vibration problem [Kaya (2006)]. A comparison was made by Kumar and Ganguli (2012) among the rotating Euler-Bernoulli beam, the rotating Timoshenko beam and the stiff-string to develop the new basis functions for the finite element formulation of the rotating beams. The violin string shape functions were developed for the rotating Timoshenko beam by Kumar and Ganguli (2011). Recently, closed form solutions for the rotating Timoshenko beam were found by Sarkar and Ganguli (2014). However, meshless methods have not found usage in the rotating Timoshenko beam literature.

The idea of the meshless methods was first introduced by Nayroles, Touzot and Villon (1992) with the diffused element method, where a smooth approximation of the field variable was considered based on the nodal distribution and the higher order derivatives were found to be continuous. The element-free Galerkin method which required a background mesh while integrating the weak form was another step towards the evolution of the meshless methods [Belytschko, Lu, and Gu (1994)]; but with the moving squares interpolation, it was difficult to apply the essential boundary conditions.

Typically, moving least squares interpolation is used with the meshless local Petrov-Galerkin method. The radial basis function interpolation is an alternative option and the application of the essential boundary conditions with the radial basis function interpolation is easier because it does satisfy the Kronecker delta property. The radial basis functions were used along with the collocation method to develop the time integration schemes and the accuracy of the method is independent of the initial guess [Elgohary, Dong, Junkins and Atluri (2014a); Elgohary, Dong, Junkins, and Atluri (2014b)]. An approximation with the combination of the polynomial basis function and the radial basis function overcomes the problem of singularity linked with the polynomial basis function approximation, and the higher order derivatives of shape functions can be easily obtained [Wang and Liu (2002)].

The meshless local Petrov-Galerkin method was successfully applied to the non-rotating and the rotating thin beam problems [Atluri, Cho, and Kim (1999); Raju, Phillips, and Krishnamurthy (2004); Panchore, Ganguli, and Omkar (2015)]. The

thin and thick plate problems were solved by Li, Soric, Jarak, and Atluri (2005), where a three dimensional locking-free meshless Petrov-Galerkin formulation was developed. The meshless Petrov-Galerkin method was mixed with the finite difference method and with the collocation method for the solid mechanics problems [Atluri, Liu, and Han (2006a); Atluri, Liu, and Han (2006b)]. A comprehensive study was carried out by Dong, Alotaibi, Mohiuddine, and Atluri (2014) where different computational methods were studied; various concepts were combined together to obtain the numerical solutions of a fourth order ordinary differential equation. This study provides simple, effective and detail explanations of meshless method and finite element method.

In the typical finite element formulation of a Timoshenko beam, the shear locking phenomenon is avoided by using a polynomial approximation of one order higher for the transverse displacement than the slope and by using the reduced integration [Reddy (2006)]. The assembly of the global matrix is a difficult task with such an approximation as the transverse displacement and the slope have different degrees of freedom within the element. The shape functions obtained by satisfying the homogenous part of the Timoshenko beam equation overcome this problem.

In the meshless method, the improvements made in the conventional finite element method domain were not addressed for the shear locking; the problem was solved with the formulation of alternate equations [Cho and Atluri (2001)] and the moving least squares interpolation was used. A similar formulation was used by Raju, Phillips, and Krishnamurthy (2004) with the radial basis function interpolation. The alternate formulation is a well thought out and elegant solution with the meshless method but the locking-free shape function formulation for the meshless method remains to be addressed.

In this paper, we derive a locking-free shape function formulation for the meshless methods using the radial basis function interpolation. For the same nodal degrees of freedom of the transverse displacement and the slope, we get higher order approximation for the transverse displacement than the slope. Results show better convergence with the locking-free approximation and avoids the shear locking associated with the normal approximation.

2 Shear locking in the timoshenko beam finite element formulation

The governing differential equations of a non-rotating Timoshenko beam are given by

$$\frac{d}{dx}\left[kGA\left(\frac{dw}{dx}-\theta\right)\right]+f=0 \tag{1}$$

$$EI\frac{d^2\theta}{dx^2} + kGA\left(\frac{dw}{dx} - \theta\right) = 0 \tag{2}$$

where, k is the shear correction factor, E is the Young's modulus, G is the shear modulus, w is the transverse displacement, A is the area of cross section and θ is the slope.

For the thin beam case, $\frac{dw}{dx} = \theta$ and using a linear interpolation of w and θ, we reach a condition that θ should be a constant, and in such a case, the bending energy $(\frac{1}{2}\int_0^R EI(d\theta/dx)^2 dx)$ will be zero. Two solutions are possible to overcome this problem: (1) Using a higher order approximation for the transverse displacement than the slope and (2) Integrating the transverse shear energy $(\frac{1}{2}\int_0^R GAk[(dw/dx) - \theta]^2 dx)$ with the reduced integration [Reddy (2006)].

For a Timoshenko beam element, Mukherjee and Prathap (2002) have discussed the delayed convergence and locking behavior with a higher order approximation. The functionally-graded beams and composite beams were modeled with a locking-alleviated 4-node mixed-collocation finite element approach [Dong, El-Gizaway, Juhany, and Atluri (2014a)] and a similar approach was used for a 3D linear elasticity problem [Dong, El-Gizaway, Juhany, and Atluri (2014b)], both of these methods were found to be superior to the existing alternatives; these methods are straight forward and computationally efficient.

3 Locking-free formulation of the Timoshenko beam for the meshless methods [Cho and Atluri (2001)]

The variational function associated with equation (1) and (2) is given by

$$\frac{1}{2}\int_0^R \left[EI\left(\frac{d\theta}{dx}\right)^2 + kGA\left(\frac{dw}{dx} - \theta\right)^2\right] dx \tag{3}$$

For the thin beam, $\frac{kGA}{EI} \to \infty, \gamma \to 0$, and $\frac{dw}{dx} - \theta \to 0$. Linear interpolation approximations for the transverse displacement and the slope are given by

$$w = a_1 + b_1 x \tag{4}$$

$$\theta = a_2 + b_2 x \tag{5}$$

Substituting equations (4) and (5) and minimization of the variational functional yields the conditions $a_2 \to b_1$ and $b_2 \to 0$. This results in zero bending energy. To overcome this problem, Cho and Atluri (2001) rewrite the variational function as

$$\frac{1}{2}\int_0^R \left[EI\left(\frac{d\theta}{dx}\right)^2 + kGA\,(\gamma)^2\right] dx \tag{6}$$

where the dependent variables are the transverse displacement (θ) and the transverse strain (γ). They write linear interpolation for θ and γ as

$$\theta = a_1 + b_1 x \tag{7}$$

$$\gamma = a_2 + b_2 x \tag{8}$$

Substituting equations (7) and (8) and minimization of the variational functional will give the conditions $a_2 \to 0$ and $b_2 \to 0$. These conditions do not lock the bending. Thus, equations (1) and (2) can be replaced with the locking-free formulation as equations (9) and (10).

$$EI\frac{d^3}{dx^3}\left(\frac{dw}{dx} - \gamma\right) - f = 0 \tag{9}$$

$$EI\frac{d^2}{dx^2}\left(\frac{dw}{dx} - \gamma\right) + kAG\gamma = 0 \tag{10}$$

4 Governing differential equations of the rotating timoshenko beam

The governing differential equations of the rotating Timoshenko beam are given as [Kaya (2006)]

$$-\rho A\frac{\partial^2 \overline{w}(x,t)}{\partial t^2} + \frac{\partial}{\partial x}\left[T(x)\frac{\partial \overline{w}(x,t)}{\partial x}\right] + \frac{\partial}{\partial x}\left\{kAG\left[\frac{\partial \overline{w}(x,t)}{\partial x} - \overline{\theta}(x,t)\right]\right\} = 0 \tag{11}$$

$$-\rho A\frac{\partial^2 \overline{\theta}(x,t)}{\partial t^2} + \rho I\Omega^2\overline{\theta}(x,t) + \frac{\partial}{\partial x}\left[EI\frac{\partial \overline{\theta}(x,t)}{\partial x}\right] + kAG\left[\frac{\partial \overline{w}(x,t)}{\partial x} - \overline{\theta}(x,t)\right] = 0 \tag{12}$$

where, ρ is the density, Ω is the angular velocity of the rotating beam, $\overline{w}$ and $\overline{\theta}$ are the transverse displacement and the slope, respectively. Here, $T(x)$ is the centrifugal force, which varies along the length of the beam and it is given as

$$T(x) = \int_x^R \rho A\Omega^2 x dx. \tag{13}$$

Substituting $\overline{w}(x,t) = e^{i\omega t}w(x)$, and $\overline{\theta}(x,t) = e^{i\omega t}\theta(x)$ in equations (11) and (12) we get

$$\rho A\omega^2 w(x) + \frac{d}{dx}\left[T(x)\frac{dw(x)}{dx}\right] + \frac{d}{dx}\left\{kAG\left[\frac{dw(x)}{dx} - \theta(x)\right]\right\} = 0 \tag{14}$$

$$\rho A\omega^2\theta(x) + \rho I\Omega^2\theta(x) + \frac{d}{dx}\left[EI\frac{d^2\theta(x)}{dx^2}\right] + kAG\left[\frac{dw(x)}{dx} - \theta(x)\right] = 0 \tag{15}$$

In non-dimensional form, for a uniform rotating Timoshenko beam we can write equations (14) and (15) as

$$\frac{d}{d\zeta}\left[\frac{(1-\zeta^2)}{2}\frac{dw(\zeta)}{d\zeta}\right]+\frac{\omega^2}{\Omega^2}w(\zeta)+\frac{1}{s^2\eta^2}\left[\frac{d^2w(\zeta)}{d\zeta^2}-\frac{d\theta(\zeta)}{d\zeta}\right] \tag{16}$$

$$\frac{d^2\theta(\zeta)}{d\zeta^2}+\eta^2r^2\left(1+\frac{\omega^2}{\Omega^2}\right)\theta(\zeta)+\frac{1}{s^2}\left[\frac{dw(\zeta)}{d\zeta}-\theta(\zeta)\right]=0 \tag{17}$$

where, $\zeta=\frac{x}{R}, w(\zeta)=\frac{w(x)}{R}$, $r^2=\frac{I}{AR^2}, s^2=\frac{EI}{kAGR^2}, \eta^2=\frac{\rho AR^4\Omega^2}{EI}$, and $\mu^2=\frac{\rho AR^4\omega^2}{EI}$.

5 Weak formulation of the rotating Timoshenko beam differential equation

The weak form of equations (16) and (17) is given as

$$\begin{aligned}&\int_{\Omega_0} v_w\frac{d}{d\zeta}\left[\frac{(1-\zeta^2)}{2}\frac{dw(\zeta)}{d\zeta}\right]d\zeta+\int_{\Omega_0} v_w\frac{\omega^2}{\Omega^2}w(\zeta)d\zeta+\int_{\Omega_0} v_w\frac{1}{s^2\eta^2}\left[\frac{d^2w(\zeta)}{d\zeta^2}-\frac{d\theta(\zeta)}{d\zeta}\right]d\zeta\\&+\int_{\Omega_0} v_\theta\frac{d^2\theta(\zeta)}{d\zeta^2}d\zeta+\int_{\Omega_0} v_\theta\eta^2r^2\left(1+\frac{\omega^2}{\Omega^2}\right)\theta(\zeta)d\zeta+\int_{\Omega_0} v_\theta\frac{1}{s^2}\left[\frac{dw(\zeta)}{d\zeta}-\theta(\zeta)\right]d\zeta\\&+\alpha_w\left[(w-\tilde{w})v_w\right]_{\Omega_0\cap\Gamma_w}+\alpha_\theta\left[(\theta-\tilde{\theta})v_\theta\right]_{\Omega_0\cap\Gamma_\theta}=0\end{aligned} \tag{18}$$

where, v_w and v_θ are the weight functions, α_w and α_θ are the penalty parameters, and Ω_0 is the complete domain.

The weak formulation can be written for a local sub-domain as

$$\begin{aligned}&-\int_{\Omega_s}\frac{dv_w}{d\zeta}\left[\frac{(1-\zeta^2)}{2}\frac{dw(\zeta)}{d\zeta}\right]d\zeta+\int_{\Omega_s} v_w\frac{\omega^2}{\Omega^2}w(\zeta)d\zeta-\int_{\Omega_s}\frac{dv_w}{d\zeta}\frac{1}{s^2\eta^2}\left[\frac{dw(\zeta)}{d\zeta}-\theta(\zeta)\right]d\zeta\\&+\int_{\Omega_s}\frac{dv_\theta}{d\zeta}\frac{d\theta(\zeta)}{d\zeta}d\zeta+\int_{\Omega_s} v_\theta\eta^2r^2\left(1+\frac{\omega^2}{\Omega^2}\right)\theta(\zeta)d\zeta+\int_{\Omega_s} v_\theta\frac{1}{s^2}\left[\frac{dw(\zeta)}{d\zeta}-\theta(\zeta)\right]d\zeta\\&+\eta_x\left[\frac{1}{s^2\eta^2}v_w\left(\frac{dw(\zeta)}{d\zeta}-\theta(\zeta)\right)+\left(\frac{1-\zeta^2}{2}\right)v_w\frac{dw(\zeta)}{d\zeta}\right]_{\Omega_s\cap\Gamma_w}\\&+\eta_x\left[v_\theta\frac{d\theta(\zeta)}{d\zeta}\right]_{\Omega_s\cap\Gamma_\theta}+\alpha_w\left[(w-\tilde{w})v_w\right]_{\Omega_s\cap\Gamma_w}+\alpha_\theta\left[(\theta-\tilde{\theta})v_\theta\right]_{\Omega_s\cap\Gamma_\theta}=0\end{aligned} \tag{19}$$

where, η_x is a unit vector and it is positive on the right hand side of the sub-domain of the nodal test function. $\Omega_s\cap\Gamma_w$ and $\Omega_s\cap\Gamma_\theta$ represent the intersection of the sub-domain of the nodal test function with the boundary, where the transverse deflection

and the slope are prescribed. The last two terms of equation (19) can be omitted where the radial basis function approximation is used.

6 Inspiration from the finite element method

In the finite element method, to avoid the shear locking, we generally use quadratic interpolation for the transverse displacement and linear interpolation for the slope, or a one order higher approximation for the transverse displacement than the slope [Reddy (2006)].

$$w(x) = a_0 + a_1 x + a_2 x^2 \tag{20}$$

$$\theta(x) = b_0 + b_1 x \tag{21}$$

The meshless approximations of the transverse displacement and the slope are given by

$$w(\zeta) = R_1(\zeta)a_1 + S_1(\zeta)b_1 + R_2(\zeta)a_2 + S_2(\zeta)b_2 + \cdots + R_N(\zeta)a_N + S_N(\zeta)b_N \tag{22}$$

$$\theta(\zeta) = R_1^{\theta}(\zeta)c_1 + R_2^{\theta}(\zeta)c_2 + \cdots + R_n^{\theta}(\zeta)c_N \tag{23}$$

where,

$$R_j(\zeta) = e^{-c\frac{(|\zeta-\zeta_j|)^2}{s_t^2}} \tag{24}$$

and

$$R_j^{(\theta)}(\zeta) = e^{-c\frac{(|\zeta-\zeta_j|)^2}{s_t^2}} \tag{25}$$

The values of c and s_t are user defined and have their impact on accuracy. Equations (24) and (25) represent normal approximations for the transverse displacement and the slope, respectively.

6.1 First locking-free approximation

Since the transverse displacement approximation should be an order higher than the slope approximation, we write the first locking-free approximation as

$$R1_j(\zeta) = \zeta e^{-c\frac{(|\zeta-\zeta_j|)^2}{s_t^2}} \tag{26}$$

Equation (26) follows a similar procedure as finite element method but at $\zeta = 0$, the first locking-free approximation $R1_j(\zeta)$ has a value zero and does not serve the purpose for all the boundary conditions. Therefore, we try to find a second locking-free approximation in the next section.

6.2 Second locking-free approximation

We write the second locking-free approximation as

$$R2_j(\zeta) = e^{-c\frac{\zeta^2(|\zeta-\zeta_j|)^2}{s_t^2}} \tag{27}$$

Equation (27) is the second locking-free approximation $R2_j(\zeta)$ and it provides a higher order approximation than the normal approximation $R_j(\zeta)$. Equations (28) and (29) show the Taylor series expansion of $R_j(\zeta)$ and $R2_j(\zeta)$ up to the first three terms, respectively.

$$\begin{aligned} R_j(\zeta) = &\left[1+\alpha\zeta_j^2+\frac{1}{2}\alpha^2\zeta_j^4\right]+\zeta\left[-2\zeta_j\alpha-2\alpha^2\zeta_j^3\right]+\zeta^2\left[\alpha+3\alpha^2\zeta_j^2\right] \\ &-2\alpha^2\zeta_j\zeta^3+\frac{1}{2}\alpha^2\zeta^4+\cdots \end{aligned} \tag{28}$$

$$\begin{aligned} R2_j(\zeta) = &1+\alpha\zeta_j^2\zeta^2-2\alpha\zeta_j\zeta^3+\zeta^4\left[\alpha+\frac{1}{2}\alpha^2\zeta_j^4\right] \\ &-2\alpha^2\zeta_j^3\zeta^5+3\alpha^2\zeta_j^2\zeta^6-2\alpha^2\zeta_j\zeta^7+\frac{1}{2}\alpha^2\zeta^8+\cdots \end{aligned} \tag{29}$$

where, $\alpha = \frac{-c}{s_t^2}$.

Equation (29) is a higher order polynomial. The term ζ^2 is multiplied within the exponential term of $R2_j(\zeta)$ for the smoothness of the curve, otherwise term ζ could have been a solution as well. $R2_j(\zeta)$ serves the purpose for the cantilever boundary condition.

In this section, equations (24), (26), and (27) represent the normal approximation, the first locking-free approximation, and the second locking-free approximation, respectively. Based on the arguments discussed, we finalize our locking-free approximation as equation (27): the second locking-free approximation $R2(\zeta)$. We follow an approach in the meshless method similar to the finite element method and use a higher order approximation for the transverse displacement relative to the slope. The numerical accuracy depends on the numerical integration.

In this paper, we will obtain the results with both these $R_j(\zeta)$ and $R2_j(\zeta)$; the results will be indicated by "Normal approximation" for equation (24) and "Locking-free approximation" for equation (27).

Note that for the hinged boundary condition, one should try $e^{-c\frac{\zeta(|\zeta-\zeta_j|)^2}{s_t^2}}$ as the locking-free approximation, where only a ζ term is multiplied within the exponential than approximation where the ζ^2 term is multiplied within the exponential of $R2_j(\zeta)$.

7 Graphical representations of the normal approximation $R_j(\zeta)$ and the locking-free approximation $R2_j(\zeta)$

Both these functions are drawn in Figures (1a)–(1f). The dotted lines show the normal radial basis approximation while continuous lines show the locking free approximation. The Figures (1a)–(1f) show a distribution over the beam of length $5m$ and 6 nodes are considered at the distance of $0m, 1m, 2m, 3m, 4m$, and $5m$, respectively.

In figures (1a)–(1f), we see that the locking-free approximation is sensitive to the increasing length of the beam and does not show a uniform distribution shown by the normal approximation. In figure (1b), we see a different behavior of the locking-free curve as $\zeta \to 0$, but the function does serve the purpose for the cantilever boundary conditions.

7.1 Shape function formulation for the transverse displacement

The transverse displacement can be approximated with the radial basis function as Raju, Phillips, and Krishnamurthy (2004)

$$w(\zeta) = R_1(\zeta)a_1 + S_1(\zeta)b_1 + R_2(\zeta)a_2 + S_2(\zeta)b_2 + \cdots + R_N(\zeta)a_N + S_N(\zeta)b_N \quad (30)$$

where, N is the number of nodes, and $a_1, b_1, a_2, b_2, \ldots, a_N, b_N$ are the arbitrary constants.

The derivative of the radial basis function is given by

$$S_j(\zeta) = \frac{dR_j(\zeta)}{dx} \quad (31)$$

We write the derivative of the transverse displacement by differentiating equation (30) with respect to ζ as

$$\begin{aligned}\frac{dw(\zeta)}{d\zeta} =& \frac{dR_1(\zeta)}{d\zeta}a_1 + \frac{dS_1(\zeta)}{d\zeta}b_1 + \frac{dR_2(\zeta)}{d\zeta}a_2 + \frac{dS_2(\zeta)}{d\zeta}b_2 \\ &+ \cdots + \frac{dR_N(\zeta)}{d\zeta}a_N + \frac{dS_N(\zeta)}{d\zeta}b_N \end{aligned} \quad (32)$$

We can rewrite the transverse displacement as

$$w(\zeta) = [Q(\zeta)]_{(1,2N)}\,[c]^T_{(2N,1)} \quad (33)$$

where,

$$[Q(\zeta)]_{(1,2N)} = [R_1\ (\zeta)\ S_1(\zeta)\ \ R_2(\zeta)\ \ S_2(\zeta)\ \ \cdots\ \ R_N(\zeta)\ \ \ S_N(\zeta)] \quad (34)$$

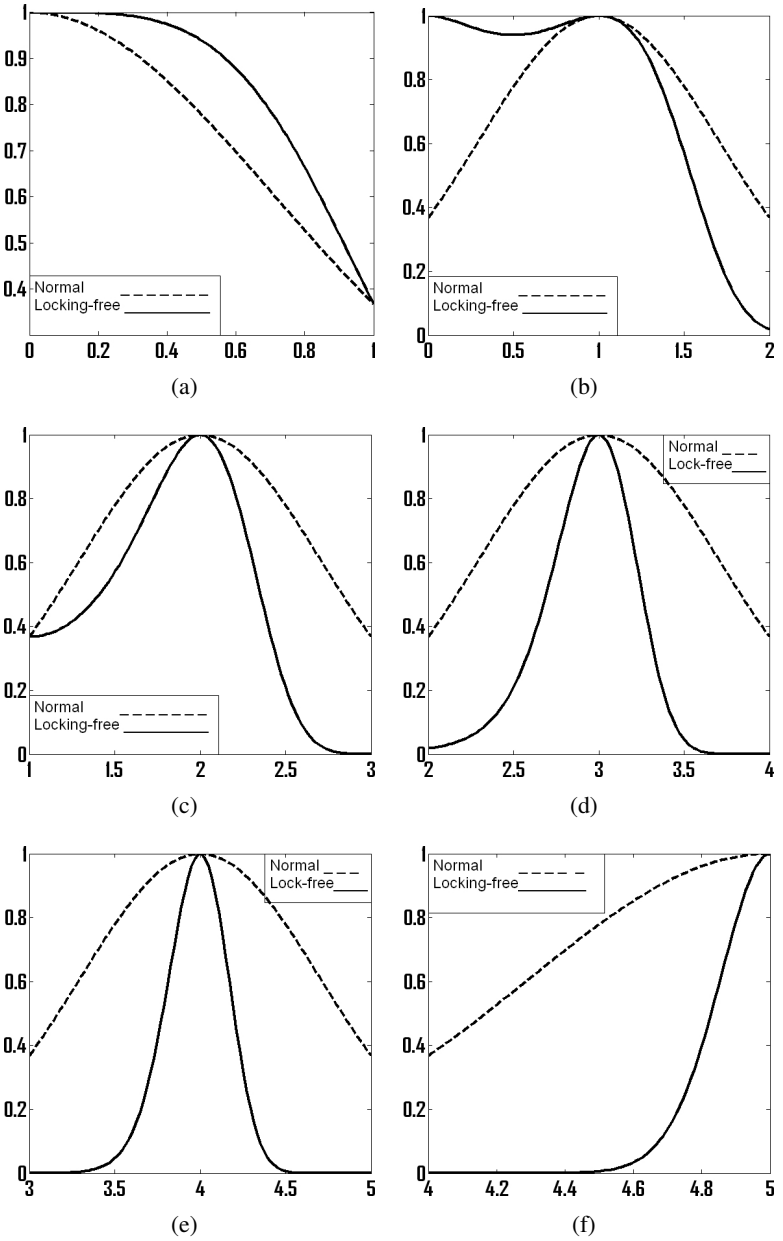

Figure 1: a and b: Variations of the approximations at nodal points 0 and 1, respectively, c and d: Variations of the approximations at nodal points 2 and 3, respectively, e and f: Variations of the approximations at nodal points 4 and 5, respectively

and

$$[c]_{(1,2N)} = [a_1 \quad b_1 \quad a_2 \quad b_2 \quad \cdots \quad a_N \quad b_N] \tag{35}$$

We can rewrite the slope as

$$\frac{dw(\zeta)}{d\zeta} = \left[\frac{dQ(\zeta)}{d\zeta}\right]_{(1,2N)} [c]^T_{(2N,1)} \tag{36}$$

where,

$$\left[\frac{dQ(\zeta)}{d\zeta}\right]_{(1,2N)} = \left[\frac{dR_1(\zeta)}{d\zeta} \quad \frac{dS_1(\zeta)}{d\zeta} \quad \frac{dR_2(\zeta)}{d\zeta} \quad \frac{dS_2(\zeta)}{d\zeta} \cdots \frac{dR_N(\zeta)}{d\zeta} \quad \frac{dS_N(\zeta)}{d\zeta}\right] \tag{37}$$

Substituting the displacement and its derivative values at the nodal points in equations (33) and (36), we get

$$[Q_M]_{(2N,2N)} [c]^T_{(2N,1)} = [d]_{(2N,1)} \tag{38}$$

where,

$$[d]^T_{(1,2N)} = \left[w_1 \quad \frac{dw_1(\zeta)}{d\zeta} \quad w_2 \quad \frac{dw_2(\zeta)}{d\zeta} \cdots w_N \quad \frac{dw_n(\zeta)}{d\zeta}\right] \tag{39}$$

and

$$[Q_M] = \begin{bmatrix} R_1(\zeta_1) & S_1(\zeta_1) & R_2(\zeta_1) & S_2(\zeta_1) & \cdots & R_N(\zeta_1) & S_N(\zeta_1) \\ \frac{dR_1(\zeta_1)}{d\zeta} & \frac{dS_1(\zeta_1)}{d\zeta} & \frac{dR_2(\zeta_1)}{d\zeta} & \frac{dS_2(\zeta_1)}{d\zeta} & \cdots & \frac{dR_N(\zeta_1)}{d\zeta} & \frac{dS_N(\zeta_1)}{d\zeta} \\ R_1(\zeta_2) & S_1(\zeta_2) & R_2(\zeta_2) & S_2(\zeta_2) & \cdots & R_N(\zeta_2) & S_N(\zeta_2) \\ \frac{dR_1(\zeta_2)}{d\zeta} & \frac{dS_1(\zeta_2)}{d\zeta} & \frac{dR_2(\zeta_2)}{d\zeta} & \frac{dS_2(\zeta_2)}{d\zeta} & \cdots & \frac{dR_N(\zeta_2)}{d\zeta} & \frac{dS_N(\zeta_2)}{d\zeta} \\ \vdots & \vdots & \vdots & \vdots & \cdots & \vdots & \vdots \\ R_1(\zeta_N) & S_1(\zeta_N) & R_2(\zeta_N) & S_2(\zeta_N) & \cdots & R_N(\zeta_N) & S_N(\zeta_N) \\ \frac{dR_1(\zeta_N)}{d\zeta} & \frac{dS_1(\zeta_N)}{d\zeta} & \frac{dR_2(\zeta_N)}{d\zeta} & \frac{dS_2(\zeta_N)}{d\zeta} & \cdots & \frac{dR_N(\zeta_N)}{d\zeta} & \frac{dS_N(\zeta_N)}{d\zeta} \end{bmatrix} \tag{40}$$

We can rewrite equation (38) as

$$[c]^T_{(2N,1)} = [Q_M]^{-1}_{(2N,2N)} [d]_{(2N,1)} \tag{41}$$

From equations (41) and (33), we get

$$w(\zeta) = [Q(\zeta)]_{(1,2N)} [Q_M]^{-1}_{(2N,2N)} [d]_{(2N,1)} \tag{42}$$

$$w(\zeta) = [N(\zeta)]_{(1,2N)} [d]_{(2N,1)} \tag{43}$$

where, $[N(\zeta)]$ is the shape function vector.

$$[N(\zeta)]_{(1,2N)} = [Q(\zeta)]_{(1,2N)} [Q_M]^{-1}_{(2N,2N)} \tag{44}$$

$$[N(\zeta)]_{(1,2N)} = \left[\phi_1^{(w)}(\zeta) \;\; \phi_1^{\left(\frac{dw}{d\zeta}\right)}(\zeta) \;\; \phi_2^{(w)}(\zeta) \;\; \phi_2^{\left(\frac{dw}{d\zeta}\right)}(\zeta) \cdots \phi_N^{(w)}(\zeta) \;\; \phi_N^{\left(\frac{dw}{d\zeta}\right)}(\zeta) \right] \tag{45}$$

where, $\phi_i^{(w)}(\zeta)$ and $\phi_i^{\left(\frac{dw}{d\zeta}\right)}(\zeta)$ are the shape functions associated with node i.
The approximate trial function can be written as

$$w(\zeta) = \sum_{j=1}^{N} (\phi_j^{(w)}(\zeta) w_j + \phi_j^{\left(\frac{dw}{d\zeta}\right)}(x) w'_j) \tag{46}$$

Figures (2a) and (2b) show the variations of the shape function and its derivative.

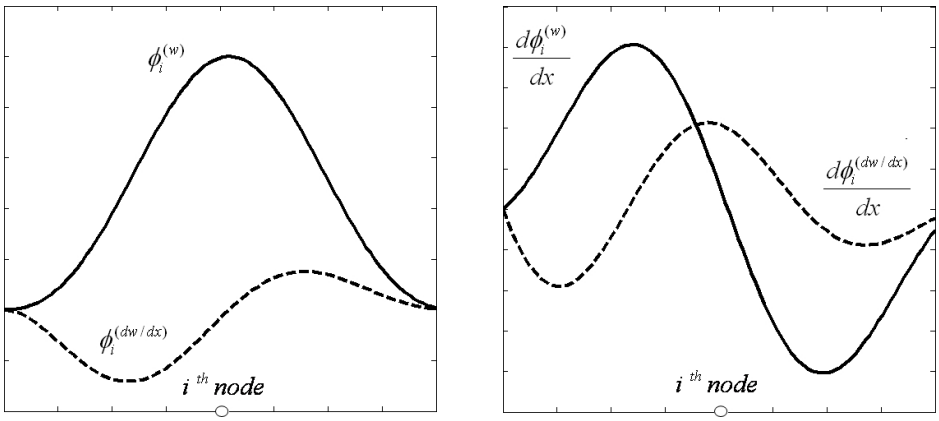

(a) (b)

Figure 2: a and b: Variations of the shape function and the shape function derivative, respectively.

7.2 Shape function formulation for the slope

$$R_j^{(\theta)}(\zeta) = e^{-c\frac{(|\zeta-\zeta_j|)^2}{s_i^2}} \tag{47}$$

Note that the length of the sub-domain of the trial function s_t and parameter c remains same for the transverse displacement and the slope approximation but basis function for the slope is of reduced order than the transverse displacement.

$$\theta(\zeta) = R_1^\theta(\zeta)c_1 + R_2^\theta(\zeta)c_2 + \cdots R_n^\theta(\zeta)c_N \tag{48}$$

We can write the slope as

$$\theta(\zeta) = \left[Q^\theta(\zeta)\right]_{(1,N)} \left[c^\theta\right]^T_{(N,1)} \tag{49}$$

where,

$$\left[Q^\theta(\zeta)\right]_{(1,N)} = \begin{bmatrix} R_1^\theta & R_2^\theta & \cdots R_N^\theta \end{bmatrix} \tag{50}$$

$$\left[c^\theta\right]_{(1,N)} = \begin{bmatrix} c_1^\theta & c_2^\theta \cdots & c_N^\theta \end{bmatrix} \tag{51}$$

Substituting the nodal values in equation (49) we get

$$\left[Q_M^\theta\right]_{(N,N)} \left[c^\theta\right]^T_{(N,1)} = \left[d^\theta\right] \tag{52}$$

where,

$$\left[Q_M^\theta\right]_{(N,N)} = \begin{bmatrix} R_1^\theta(\zeta_1) & R_2^\theta(\zeta_1) & \ldots & R_N^\theta(\zeta_1) \\ R_1^\theta(\zeta_2) & R_2^\theta(\zeta_2) & \ldots & R_N^\theta(\zeta_2) \\ \vdots & \vdots & \ldots & \vdots \\ R_1^\theta(\zeta_N) & R_2^\theta(\zeta_N) & \ldots & R_N^\theta(\zeta_N) \end{bmatrix} \tag{53}$$

$$\left[d^\theta\right]^T_{(1,N)} = [\theta_1 \quad \theta_2 \quad \cdots \quad \theta_N] \tag{54}$$

From equations (52) and (49) we can write

$$\theta(\zeta) = \left[Q^\theta(\zeta)\right]_{(1,N)} \left[Q_M^\theta\right]^{-1}_{(N,N)} \left[d^\theta\right]^T_{(N,1)} \tag{55}$$

The shape function for the slope can be written as

$$[H(\zeta)]_{(1,N)} = \left[Q^\theta(\zeta)\right]_{(1,N)} \left[Q_M^\theta\right]^{-1}_{(N,N)} \tag{56}$$

$$[H(\zeta)]_{(1,N)} = \left[\phi_1^\theta(\zeta) \;\; \phi_2^\theta \;\; (\zeta) \cdots \phi_N^\theta(\zeta)\right] \tag{57}$$

Where, $\phi_i^{(\theta)}(\zeta)$ is the shape functions associated with node i, and the slope can be approximated as

$$\theta(\zeta) = \sum_{j=1}^{N} \phi_j^{(\theta)}(\zeta)\theta_j \tag{58}$$

Figures (3a) and (3b) show the variation of the shape function and its derivative.

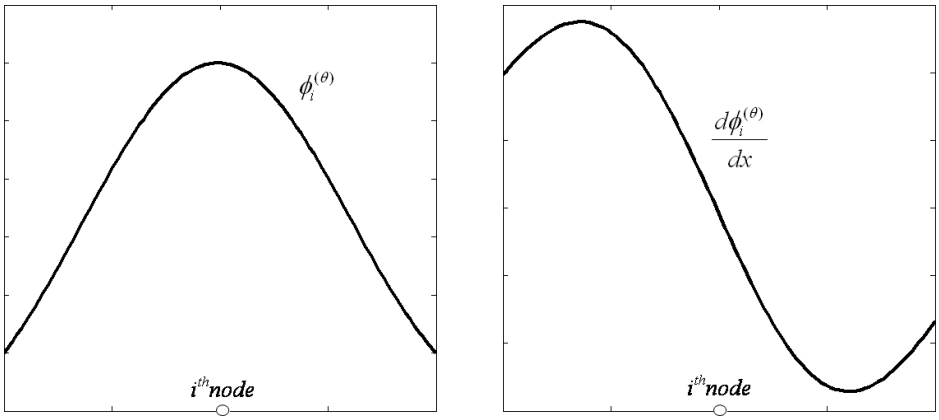

(a) (b)

Figure 3: a and b: Variations of the shape function (slope) and the shape function derivative, respectively.

8 Test functions for the meshless local Petrov-Galerkin method

Basis function for the test function can be chosen arbitrarily such that it is zero outside the sub-domain of the nodal test function and it is given by Raju, Phillips, and Krishnamurthy (2004)

$$\chi_i^{(w)}(\zeta) = \begin{cases} \left[1 - \left(\frac{|\zeta-\zeta_i|}{s_v}\right)^2\right]^4 & 0 \le |\zeta - \zeta_i| \le s_v \\ 0 & |\zeta - \zeta_i| > s_v \end{cases} \tag{59}$$

$$\chi_i^{\left(\frac{dw}{d\zeta}\right)} = \frac{d\chi^{(w)}(\zeta)}{d\zeta} \tag{60}$$

where, $\chi_i^{(w)}(\zeta)$ and $\chi_i^{\left(\frac{dw}{d\zeta}\right)}(\zeta)$ are the basis functions for node i, ζ_i is the spatial location of the node and $2s_v$ is the sub-domain length of the test function given by

$$v_w = \delta w_i \chi_i^{(w)}(\zeta) + \delta w_i' \chi_i^{\left(\frac{dw}{d\zeta}\right)}(\zeta) \tag{61}$$

For the slope approximation, we write

$$\chi_i^{(\theta)}(\zeta) = \begin{cases} \left[1 - \left(\frac{|\zeta-\zeta_i|}{s_v}\right)^2\right]^2 & 0 \le |\zeta - \zeta_i| \le s_v \\ 0 & |\zeta - \zeta_i| > s_v \end{cases} \tag{62}$$

where, $\chi_i^{(\theta)}(\zeta)$ is the basis function for node i.

$$v_\theta = \delta\theta_i \chi_i^{(\theta)}(\zeta) \tag{63}$$

Figures (4a) and (4b) show the variations of basis functions for the transverse displacement and the slope, respectively. Where, d is the distance between the two consecutive nodes. Two curves are shown for the sub-domain length of the test function $2d$ and $4d$. Figure (5) shows the overlapping of the sub-domains of the test functions.

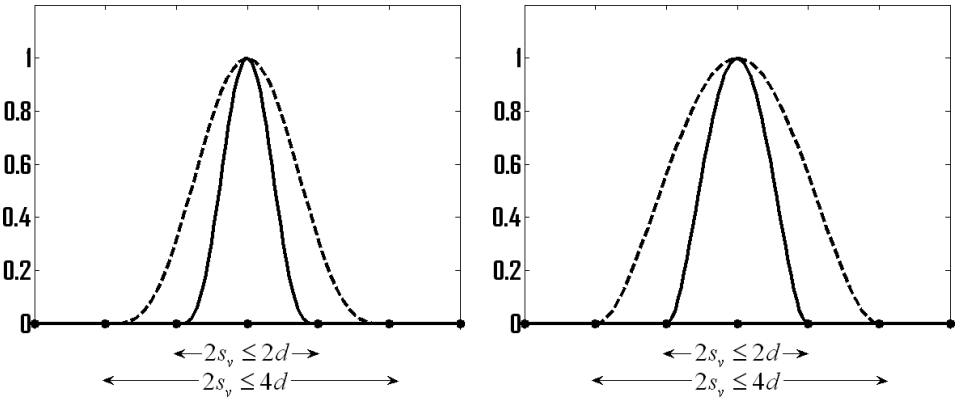

Figure 4: a and b: Variations of test functions within the sub-domain for transverse displacement and slope, respectively.

9 Meshless local petrov-galerkin formulation

Based on the weak form of the problem, the algebraic equations can be written for each nodal test function. One advantage the meshless method shows over the conventional finite element method is that for a higher order approximation of the transverse displacement than the slope, we get the same degrees of freedom over the complete domain, while in the finite element approximation, we get the higher degrees of freedom for the transverse displacement within the element. From equations (19), (46), (58), (61), and (63) we write the equation for the i^{th} sub-domain of the test function.

$$\omega^2 [M]^{(node)}[\phi] = ([K]^{(node)} + [K]^{(bound)})[\phi] \tag{64}$$

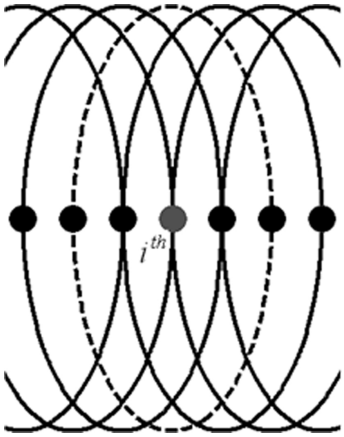

Figure 5: Overlapping of the sub-domains of the test functions, sub-domain of the i^{th} node in dotted line.

For the i^{th} node, we write the mass matrix as

$$[M]^{(i^{\text{th}}\ node)} = \begin{bmatrix} \int\limits_{\Omega_s^{(i)}} \frac{1}{\Omega^2} \begin{bmatrix} \chi_i^{(w)} \\ \chi_i^{\left(\frac{dw}{d\zeta}\right)} \end{bmatrix}_{(2,1)} [N(\zeta)]_{(1,2N)} d\zeta & [0]_{(1,2N)} \\ [0]_{(2,N)} & \int\limits_{\Omega_s^{(i)}} \frac{r^2}{\Omega^2} [\chi_i^{(\theta)}]_{(1,1)} [H(\zeta)]_{(1,N)} d\zeta \end{bmatrix}_{(3,3N)} \tag{65}$$

and the stiffness matrix as

$$[K]^{(i^{\text{th}}\ node)} = \begin{bmatrix} [A_1]_{(2,2N)} & [A_2]_{(2,N)} \\ [A_3]_{(1,2N)} & [A_4]_{(1,N)} \end{bmatrix}_{(3,3N)} \tag{66}$$

where,

$$[A_1] = \int\limits_{\Omega_s^{(i)}} \frac{1}{s^2\eta^2} \begin{bmatrix} \frac{d\chi_i^{(w)}}{d\zeta} \\ \frac{d\chi_i^{\left(\frac{dw}{d\zeta}\right)}}{d\zeta} \end{bmatrix}_{(2,1)} \left[\frac{d[N(\zeta)]}{d\zeta}\right]_{(1,2N)} d\zeta$$
$$+ \int\limits_{\Omega_s^{(i)}} \left(\frac{1-\zeta^2}{2}\right) \begin{bmatrix} \frac{d\chi_i^{(w)}}{d\zeta} \\ \frac{d\chi_i^{\left(\frac{dw}{d\zeta}\right)}}{d\zeta} \end{bmatrix}_{(2,1)} \left[\frac{d[N(\zeta)]}{d\zeta}\right]_{(1,2N)} d\zeta,$$

$$[A_2] = -\int_{\Omega_s^{(i)}} \frac{1}{s^2\eta^2} \begin{bmatrix} \frac{d\chi_i^{(w)}}{d\zeta} \\ \left(\frac{dw}{d\zeta}\right) \\ \frac{d\chi_i}{d\zeta} \end{bmatrix}_{(2,1)} [H(\zeta)]_{(1,N)}\, d\zeta,$$

$$[A_3] = -\int_{\Omega_s^{(i)}} \frac{1}{s^2\eta^2} \left[\chi_i^{(\theta)}\right]_{(1,1)} \left[\frac{d[N(\zeta)]}{d\zeta}\right]_{(1,2N)} d\zeta,$$

and

$$[A_4] = \int_{\Omega_s^{(i)}} \frac{1}{\eta^2} \left[\frac{d\chi_i^{(\theta)}}{d\zeta}\right]_{(1,1)} \left[\frac{d[H(\zeta)]}{d\zeta}\right]_{(1,N)} d\zeta + \int_{\Omega_s^{(i)}} \frac{1}{s^2\eta^2} \left[\chi_i^{(\theta)}\right]_{(1,1)} [H(\zeta)]_{(1,N)} - \int_{\Omega_s^{(i)}} r^2 \left[\chi_i^{(\theta)}\right]_{(1,1)} [H(\zeta)]_{(1,N)}\, d\zeta$$

Nodes contributing to the boundary will give the additional stiffness term as

$$[K]^{(bound)} = \begin{bmatrix} [b_1] & [b_2] \\ [b_3] & [b_4] \end{bmatrix} \tag{67}$$

where,

$$[b_1] = -\frac{1}{s^2\eta^2} \begin{bmatrix} \chi_i^{(w)} \\ \chi_i^{\left(\frac{dw}{dx}\right)} \end{bmatrix}_{(2,1)} \left[\frac{d[N(\zeta)]}{d\zeta}\right]_{(1,2N)} - \left(\frac{1-\zeta^2}{2}\right) \begin{bmatrix} \chi_i^{(w)} \\ \chi_i^{\left(\frac{dw}{dx}\right)} \end{bmatrix}_{(2,1)} \left[\frac{d[N(\zeta)]}{d\zeta}\right]_{(1,2N)},$$

$$[b_2] = \frac{1}{s^2\eta^2} \begin{bmatrix} \chi_i^{(w)} \\ \chi_i^{\left(\frac{dw}{dx}\right)} \end{bmatrix}_{(2,1)} [H(\zeta)]_{(1,N)},$$

$[b_3] = [0]_{(1,2N)}$, and

$$[b_4] = -\frac{1}{\eta^2} \left[\chi_i^{(\theta)}\right]_{(1,1)} \left[\frac{d[H(\zeta)]}{d\zeta}\right]_{(1,N)}.$$

We can write the free vibration problem in a matrix form as

$$\omega^2 [M]^{i^{\text{th}}\ node}_{(3,3N)} \begin{bmatrix} [w]_{(2N,1)} \\ [\theta]_{(N,1)} \end{bmatrix} = \left([K]^{i^{\text{th}}\ node}_{(3,3N)} + [K]^{(bound)}_{(3,3N)}\right) \begin{bmatrix} [w]_{(2N,1)} \\ [\theta]_{(N,1)} \end{bmatrix} \tag{68}$$

Equation (68) contains the local mass and the local stiffness matrix for a single sub-domain of the test function. Writing equations for all the sub-domains of the test function, we get

$$\omega^2 [M_G]_{(3N,3N)} \begin{bmatrix} [w]_{(2N,1)} \\ [\theta]_{(N,1)} \end{bmatrix} = [K_G]_{(3N,3N)} \begin{bmatrix} [w]_{(2N,1)} \\ [\theta]_{(N,1)} \end{bmatrix} \tag{69}$$

where, $[M_G]$ and $[K_G]$ are the global mass and the global stiffness matrices. The natural frequencies can be calculated with the direct application of the essential boundary condition.

Table 1: Non-dimensional fundamental frequency of a rotating Timoshenko beam for different non dimensional rotating speeds (η).

$r = \frac{1}{30}$ and $\frac{E}{kG} = 3.059$		
η	Baseline [Kaya (2006)]	Locking-free Approximation $p = 7$
0	3.4798	3.4890
1	3.6445	3.6543
2	4.0971	4.1069
3	4.7516	4.7618
4	5.5314	5.5428
5	6.3858	6.3991
10	11.0643	11.0986

Table 2: Non-dimensional natural fundamental frequency at $\eta = 0$, for different values of Timoshenko parameter (r).

$\eta = 0$, $\frac{E}{G} = \frac{8}{3}$, and $k = \frac{2}{3}$			
r	Baseline [Kaya (2006]	Locking-free Approximation $p = 7$	Normal Approximation $p = 7$
0.001	3.5160	3.4900	$15.5381i$
0.01	3.5119	3.5210	3.1067
0.1	3.1738	3.1806	3.1754
0.15	2.8692	2.8737	2.8710

10 Results and discussion

The Timoshenko rotating beam free vibration results are shown in Tables (1)–(5). Results in Tables (2)–(5) clearly show that the locking free shape function formulation is better than the normal shape function formulation. We use 7 nodes in one sub-domain length of the trial function. Table (1) shows the non-dimensional fundamental natural frequency for varying non-dimensional rotating speeds, where, p is the number of nodes in one sub-domain length of the trial function.

Table 3: Non-dimensional natural fundamental frequency at $\eta = 4$, for different values of Timoshenko parameter (r).

$\eta = 4,\ \frac{E}{G} = \frac{8}{3}$, and $k = \frac{2}{3}$			
r	Baseline [Kaya (2006]	Locking-free Approximation $p = 7$	Normal Approximation $p = 7$
0.001	5.5850	5.6129	$15.2516i$
0.01	5.5791	5.5893	5.3330
0.1	5.1448	5.1658	5.1621
0.15	4.8262	4.8518	4.8503

Table 4: Non-dimensional natural fundamental frequency at $\eta = 8$, for different values of Timoshenko parameter (r).

$\eta = 8,\ \frac{E}{G} = \frac{8}{3}$, and $k = \frac{2}{3}$			
r	Baseline [Kaya (2006]	Locking-free Approximation $p = 7$	Normal Approximation $p = 7$
0.001	9.2568	9.3568	$13.9329i$
0.01	9.2447	9.2642	9.1056
0.1	8.5735	8.6200	8.6184
0.15	8.1406	8.1886	8.1885

Tables (2)–(5) show the non-dimensional fundamental natural frequency for the varying non-dimensional rotating speeds and for the varying Timoshenko parameter values. We get shear locking when $r \to 0$, and it is observed with the normal radial basis function approximation, where we get complex eigenvalues. The locking-free approximation avoids the shear locking and we get accurate values of the non-dimensional frequencies.

Table 5: Non-dimensional natural fundamental frequency at $\eta = 12$, for different values of Timoshenko parameter (r).

$\eta = 12,\ \frac{E}{G} = \frac{8}{3}$, and $k = \frac{2}{3}$			
r	Baseline [Kaya (2006]	Locking-free Approximation $p = 7$	Normal Approximation $p = 7$
0.001	13.170	13.3278	$10.8293i$
0.01	13.148	13.1881	13.0726
0.1	12.247	12.3228	12.3231
0.15	11.398	11.4582	11.4574

11 Conclusion

A locking-free shape function formulation is obtained for the meshless local Petrov-Galerkin method using the radial basis function. The locking-free approximation avoids the ill conditioning associated with the normal approximation. The current work encourages the use of the locking free shape function formulation for other meshless basis functions and permits keeping the governing differential equation of a Timoshenko beam unchanged. Results are validated for the fixed-free boundary condition and show good agreement with existing literature.

References

Atluri, S. N. (2004): *The Meshless Method (MLPG) for Domain and BIE Discretizations.* Tech Science Press, Forsyth.

Alturi, S. N.; Cho, J. Y.; Kim, H.-G. (1999): Analysis of the beams, using the meshless local Petrov-Galerkin method, with generalized moving least squares interpolations. *Computational Mechanics*, vol. 24, pp. 334–347.

Atluri, S. N.; Liu, H. T.; Han, Z. D. (2006a): Meshless local Petrov-Galerkin mixed collocation method for elasticity problems. *Computer Modeling in Engineering and Sciences*, vol. 14, pp. 141–152.

Atluri, S. N.; Liu, H. T.; Han, Z. D. (2006b): Meshless local Petrov-Galerkin mixed finite difference method for solid mechanics problems. *Computer Modeling in Engineering and Sciences*, vol. 15, pp. 1–16.

Atluri, S. N.; Shen, S. (2002): *The Meshless Local Petrov-Galerkin Method.* Tech Science Press, Forsyth, GA.

Banerjee, J. R. (2001): Dynamic stiffness formulation and free vibration analysis of centrifugally stiffened Timoshenko beams. *Journal of Sound and Vibration*, vol. 247, pp. 97–115.

Belytschko, Y.; Lu, Y. Y.; Gu, L. (1994): Element-free Galerkin methods. *International Journal for Numerical Methods in Engineering*, vol. 37, pp. 229–256.

Cho, J. Y.; Atluri, S. N. (2001): Analysis of shear flexible beams, using the meshless local Petrov-Galerkin method, based on a locking-free formulation. *Engineering Computations*, vol. 18, pp. 215–240.

Dong, L.; Alotaibi, A.; Mohiuddine, S. A.; Atluri, S. N. (2014): Computational methods in engineering: a variety of primal and mixed methods, with global and local interpolations, for well-posed or ill-posed boundary conditions. *Computer Modeling in Engineering and Sciences*, vol. 100, pp. 249–275.

Dong, L.; El-Gizawy, A. S.; Juhany, K. A.; Atluri S. N. (2014a): A simple locking-alleviated 4-node mixed-collocation finite element with over-integration, for homogeneous or functionally-graded or thick-section laminated composite beams. *Computers, Materials & Continua*, vol. 40, pp. 49–77.

Dong, L.; El-Gizawy, A. S.; Juhany, K. A.; Atluri S. N. (2014b): A simple locking-alleviated 3D 8-node mixed-collocation C^0finite element with over-integration, for functionally-graded and laminated thick-section plates an shells, with and without z-pins. *Computers, Materials & Continua*, vol. 41, pp. 163–192.

Du, H.; Lim, M. K.; Liew, K. M. (1994): A power series solution for vibration of a rotating Timoshenko beam. *Journal of Sound and Vibration*, vol. 175, pp. 505–523.

Elgohary, T. A.; Dong, L.; Junkins, J. L.; Atluri, S. N. (2014a): Time domain inverse problems in nonlinear systems using collocation and radial basis functions. *Computer Modeling in Engineering and Sciences*, vol. 100, pp. 59–84.

Elgohary, T. A.; Dong, L.; Junkins, J. L.; Atluri, S. N. (2014b): A simple, fast, and accurate time-integrator for strongly nonlinear dynamical systems. *Computer Modeling in Engineering and Sciences*, vol. 100, pp. 249–275.

Kaya, O. M. (2006): Free vibration analysis of a rotating Timoshenko beam by differential transform method. *Aircraft Engineering and Aerospace Technology: An International Journal*, vol. 78, pp. 194–203.

Kumar, A. S. V.; Ganguli, R. (2012): Analogy between rotating Euler-Bernoulli and Timoshenko beams and stiff strings. *Computer Modeling in Engineering and Sciences*, vol. 1639, pp. 1–32.

Kumar, A. S. V.; Ganguli, R. (2011): Violin string shape functions for finite element analysis of rotating Timoshenko beams. *Finite Elements in Analysis and Design*, vol. 47, pp. 1091–1103.

Li, Q.; Soric, J.; Jarak, T.; Atluri, S. N. (2005): A locking-free meshless local Petrov-Galerkin formulation for thick and thin plates. *Journal of Computational Physics*, vol. 208, pp. 116–133.

Mukherjee, S.; Prathap, G. (2002): Analysis of delayed convergence in the three-nodes Timoshenko beam element using the function space approach. *Sadhana*, vol. 27, pp. 507–526.

Nayroles, B.; Touzot, G.; Villon, P. (1992): Generalizing the finite element method: Diffuse approximation and diffuse elements. *Computational Mechanics*, vol. 10, pp. 307–318.

Ozgumus, O. O.; Kaya, M. O. (2010): Vibration analysis of a rotating tapered Timoshenko beam using DTM. *Meccanica*, vol. 45, pp. 333–42.

Panchore, V.; Ganguli, R.; Omkar, S. N. (2015): Meshless local Petrov-Galerkin method for rotating Euler-Bernoulli beam. *Computer Modeling in Engineering and Sciences*, vol. 104, pp. 353–373.

Raju, I. S.; Phillips, D. R. (2004): Radial basis meshless local Petrov-Galerkin method for thick beams. *AIAA*, pp. 2004–1768.

Raju, I. S.; Phillips, D. R.; Krishnamurthy, T. (2004): A radial basis function approach in the meshless local Petrov-Galerkin method for Euler-Bernoulli beam problems. *Computational Mechanics*, vol. 34, pp. 464–474.

Rao, S. S.; Gupta, R. S. (2001): Finite element vibration analysis of rotating Timoshenko beams. *Journal of Sound and Vibration*, vol. 242, pp. 103–124.

Reddy, J. N. (2006): *An Introduction to the Finite Element Method.* Tata McGraw-Hill, New York.

Sarkar, K.; Ganguli, R. (2014): Analytical test functions for free vibration analysis of rotating non-homogeneous Timoshenko beams. *Meccanica*, vol. 49, pp. 1469–1477.

Sladek, J.; Stanak, P.; Han, Z-D.; Sladek, V.; Alturi, S. N. (2013): Applications of the MLPG method in engineering and sciences: A review. *Computer Modeling in Engineering and Sciences*, vol. 92, pp. 423–475.

Stafford, R. O.; Giurgiutiu, V. (1975): Semi-analytical methods for rotating Timoshenko beams. *International Journal of Mechanical Sciences*, vol. 17, pp. 719–727.

Wang, J. G.; Liu, G. R. (2002): A point interpolation meshless method based on radial basis functions. *International Journal for Numerical Methods in Engineering*, vol. 54, pp. 1623–1648.

Xiao, J. R.; McCarthy, M. A. (2003): Meshless analysis of Timoshenko beams based on a locking-free formulation and variational approaches. *Computer Methods in Applied Mechanics and Mechanical Engineering*, vol. 192, pp. 4403–4424.

Yokoyama, T. (1987): Free vibration characteristics of rotating Timoshenko beams. *International Journal of Mechanical Sciences*, vol. 30, pp. 743–755.